

## RESEARCH ARTICLE - APPLICATION

# An optimized procedure to develop a 3-dimensional microfluidic hydrogel with parallel transport networks

Mahboubeh Jafarkhani<sup>1,2</sup> | Zeinab Salehi<sup>1</sup>  | Mohammad Ali Shokrgozar<sup>3</sup> | Shohreh Mashayekhan<sup>4</sup>

<sup>1</sup>School of Chemical Engineering, College of Engineering, University of Tehran, Tehran, Iran

<sup>2</sup>Department of Micro- and Nanotechnology, Technical University of Denmark, Kgs. Lyngby 2800, Denmark

<sup>3</sup>National Cell Bank of Iran, Pasteur Institute of Iran, Tehran, Iran

<sup>4</sup>Department of Chemical and Petroleum Engineering, Sharif University of Technology, Tehran, Iran

## Correspondence

Zeinab Salehi, School of Chemical Engineering, College of Engineering, University of Tehran, Tehran, Iran.  
Email: zsalehy@ut.ac.ir

## Funding information

Iranian National Science Foundation (INSF)

## Abstract

The development of microfluidic hydrogels is an attractive method to generate continuous perfusion, induce vascularization, increase solute delivery, and ultimately improve cell viability. However, the transport processes in many in vitro studies still have not been realized completely. To address this problem, we have developed a microchanneled hydrogel with different collagen type I concentrations of 1, 2, and 3 wt% and assessed its physical properties and obtained diffusion coefficient of nutrient within the hydrogel. It is well known that microchannel geometry has critical role in maintaining stable perfusion rate. Therefore, in this study, a computational modeling was applied to simulate the 3D microfluidic hydrogel and study the effect of geometric parameters such as microchannel diameters and their distance on the nutrient diffusion. The simulation results showed that the sample with 3 channels with a diameter of 300  $\mu\text{m}$  has adequate diffusion rates and efficiency (56%). Moreover, this system provides easy control and continuous perfusion rate during 5 days of cell culturing. The simulation results were compared with experimental data, and a good correlation was observed for nutrient profiles and cell viability across the hydrogel.

## KEYWORDS

3D tissue engineering, microfluidic hydrogel, numerical study, nutrient transfer

## 1 | INTRODUCTION

Microfabrication techniques have emerged as an attractive method to create perfusion to form a widespread network of microchannels within hydrogels and stimulate vascularization.<sup>1,2</sup> Moreover, the presence of an extensive network allows precise control for dynamic cultures and enhance the in vitro cell functionality by imitating the complexities of tissue structure when compared to static cultures.<sup>3</sup>

It is well known that an ideal hydrogel should provide a rich environment of nutrients and improve cell proliferation and reduce cell death.<sup>4</sup> By embedding microfluidic channels within the hydrogels, instant perfusion of culture media can be created and cell viability will be improved.<sup>5,6</sup> Indeed, microfabrication techniques are great tools to facilitate nutrient transfer in the hydrogel constructs and ultimately generate a functional tissue.<sup>7</sup> For example, in some studies, microchannels were embedded in agarose hydrogel to provide nutrients to the cells and induce vascularization.<sup>8,9</sup> According to the strong correlation between cell viability and the nutrient distribution, it is necessary to examine the

nutrient and soluble factor distributions in the hydrogel bulk. Song et al<sup>10</sup> developed a 3D model to study the effect of different microchannel diameter and channel-to-channel distance on nutrient transport and cell viability. They also reported that to optimize the perfusion, it is necessary to take into account nutrient consumption by the cells.

Numerical modeling of microfluidic systems was first utilized in 1976 to study the effect of tumor angiogenic factor on the growth capillary structures in melanomas and provide differential equations to predict tumor growth as a function of vessel density and concentration of tumor angiogenic factor.<sup>11</sup> Numerical studies have been developed to understand the effect of fluid flow in the microchannels on cell behaviors during tissue regeneration. Therefore, in few studies, numerical studies have been accomplished for microfluidic systems.<sup>12–14</sup> These numerical studies presented the profile of velocity, flow fields, pressure, shear stresses, and solute transfer in cell culturing chambers.<sup>15</sup> Thus, numerical studies are very beneficial tools to develop the optimum design of internal geometric configurations of microchannels in the cell cultures.

For instance, Lawrence et al<sup>16</sup> investigated the influence of cell culture geometry on flow fields applying a computational fluid dynamics software (COMSOL Multiphysics). They applied Brinkman equation to model the permeability characteristics inside the chitosan scaffolds. They reported that by pore size reduction, the fluid flow and nutrient transport were limited and significant enhancement of pressure was observed.

In this study first, we fabricated a 3D microengineered hydrogel via an efficient and simple molding method and studied the effect of collagen concentration on physical properties, permeability, and hydraulic conductivity of the hydrogel and obtained diffusion coefficient of nutrients within the culture media. Using the result, we simulated a stably perfused collagen microfluidic system contained a parallel array of perfusion channels of 3 different diameters (100, 300, 500  $\mu\text{m}$ ). Then, we determined how channel diameter and interchannel separation influence on nutrient transfer and in consequence cell viability. These numerical results can then be applied to define optimum dimensions of the channels and to predict the experimental cell viability data. The importance of this study is to investigate the influence of different effective parameters on endothelial cell behaviors in a microfluidic system and obtain the optimum conditions.

## 2 | MATERIALS AND METHODS

### 2.1 | Materials

Bovine collagen (type I, purified, and extracted from skin) and human umbilical vein endothelial cells (HUVECs) and its specific culture media were purchased from Sigma-Aldrich. Culture media and additive components were bought from Gibco-Invitrogen, CA. Glutaraldehyde and FITC-dextran (0.25 mM, 20 kDa) were obtained from Fluka Chemika and Sigma-Aldrich respectively.

### 2.2 | Formation of microfluidic hydrogel

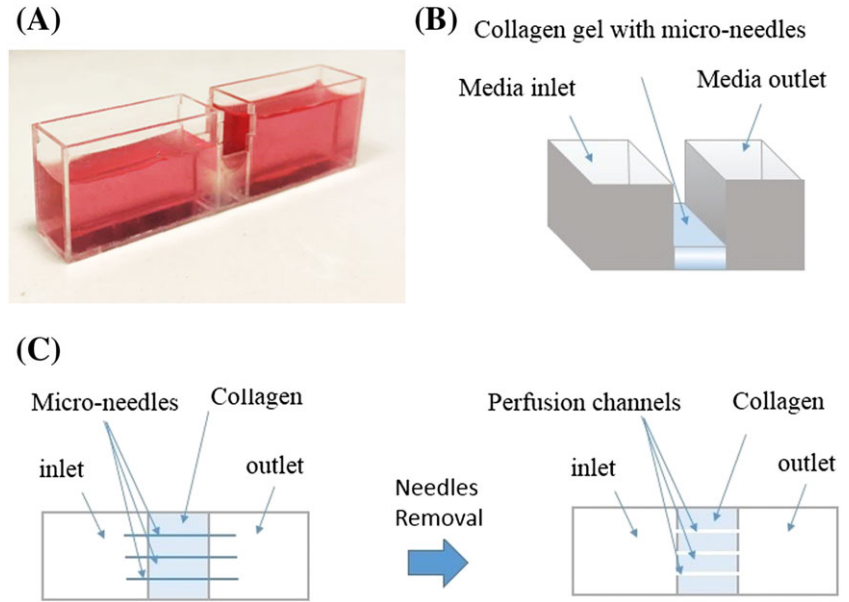
A channeled hydrogel of collagen was fabricated via a simple method using microneedles as shown in Figure 1A,B. Briefly, collagen at varying concentrations of 1, 2, and 3 wt% was dissolved in HCL 1% (v/v) solution. By NaOH addition, pH of the solution was increased to 7.4 and then mixed with 1 mL of the cell suspension ( $2 \times 10^7$  cells/mL) and finally poured into a cubic polycarbonate (PMMA) mold (a chamber with 0.7 cm  $\times$  0.9 cm  $\times$  0.5 cm) and then was incubated at 37°C for 2 hours for gelation. To create the microchannel within the hydrogel, a certain number (1, 3, and 5) of microneedles with the diameters of 100, 300, and 500  $\mu\text{m}$  had been inserted in the PMMA mold. After the collagen gelation (~20 minutes), the microneedles were removed from the PMMA mold to generate the microchannel (Figure 1C). The continuous flow (with an average of 25 mL/minute during 2 days) of culture media in the collagen microchannel was created via hydrostatic pressure difference between the inlet and outlet reservoirs. The perfusion of the cultures was implemented inside microchannels within the CO<sub>2</sub> incubator. We renewed the culture medium every 2 days.

### 2.3 | Hydrogel characterization

#### 2.3.1 | Scanning electron microscopy (SEM)

To monitor the microstructural properties of collagen hydrogels, SEM (AIS2100, South Korea) observation was used. Briefly, the dried and porous samples were cut and coated with platinum and gold and observed under at voltage of 15 kV.

**FIGURE 1** A, A photograph of the PMMA device and collagen gel in the middle chamber and culture media inside the reservoirs. B, A schematic of the microfluidic system. C, An illustration of the fabrication of microfluidic hydrogels; the prepared hydrogels of collagen (1–3 wt%) and HUVECs ( $10^7$  cells/mL) were mixed at  $37^\circ\text{C}$  and poured in the middle chamber of microfluidic device containing microneedles. The culture media were poured in both inlet and outlet reservoirs up to certain level mixture. After incubation for 2 hours and collagen gelation, the microneedles were removed from the chamber to generate the microchannels to provide medium perfusion due to the hydrostatic pressure difference



### 2.3.2 | Permeability quantification and hydraulic conductivity

The permeability of the collagen microfluidic gel was measured using Darcy's law, which shows the relation between liquid flow rate and the pressure difference between inlet and outlet reservoirs. Therefore, the hydrogels within the PMMA devices were exposed to a pressure gradient, and the permeability was measured. The initial media columns' height difference on both sides of the collagen gel, which caused a pressure gradient, was 13 mm  $\text{H}_2\text{O}$ . Based on Darcy's law the permeability is counted as follows:

$$\Delta P(t) = \Delta P(0) \cdot e^{-ct} \quad (1)$$

where  $\Delta P(t)$  is the pressure difference at time  $t$ ,  $\Delta P(0)$  presents the initial pressure difference, and  $c$  is a constant which is related to the permeability ( $K$ ) as the following equation:

$$K = \frac{c \cdot \mu \cdot L \cdot A_r}{\rho \cdot g \cdot A} \quad (2)$$

where  $\mu$ ,  $L$ ,  $g$ , and  $\rho$  are the culture media viscosity, gel length, gravity, and culture media density respectively. Moreover,  $A_r$  and  $A$  are the areas of the media reservoirs and the cross-sectional area of the channels respectively.<sup>17</sup>

Hydraulic conductivities of the samples were measured based on Wong et al method.<sup>18</sup> The cubical collagen gels were subjected to a certain pressure gradient, and the resulting flow of perfusion media was measured. Hydraulic conductivity ( $H_{cond.}$ ) was obtained by the following equation:

$$H_{cond.} = \frac{QL}{A_g \Delta P} \quad (3)$$

where  $Q$  is flow rate (about 10–35 mL/minute),  $L$  is the gel length (7 mm),  $A_g$  is the cross-sectional area of the gel ( $0.5 \text{ cm}^2$ ), and  $\Delta P$  is the pressure gradient (13–4 mm  $\text{H}_2\text{O}$ ). Several pressure differences were used to calculate hydraulic conductivity for each sample.

### 2.3.3 | Diffusion quantification

Pore control diffusion profiles of nutrients from the microchannel to the microfluidic hydrogel bulk were. We studied the diffusion patterns inside the collagen gels by using a fluorescent dye (FITC-dextran) which has approximately an equal molecular weight to the metabolic growth factors in the body. Therefore, the diffusion profiles were characterized over time for each sample having various collagen concentrations by performing diffusion experiments at  $37^\circ\text{C}$  to let

FITC-dextran infuse into the hydrogel's bulk by the pure diffusion mechanism. To analyze the diffusion profiles in collagen gels, we used an inverted fluorescent microscope and ImageJ software.

## 2.4 | Cell culture

HUVECs and its specific culture media were bought from Sigma-Aldrich. Cells were retained until they reached to 80% confluence in an incubator at 37°C with a wet atmosphere of 95% air and 5% CO<sub>2</sub>. HUVECs below passage 7 were used for this study. HUVECs were encapsulated inside the collagen gels, and then, culture media were perfused through the channels.

## 2.5 | Cell viability analysis

We studied cell viability in the microfluidic hydrogels using calcein AM and ethidium homodimer-1 (EthD-1) to stain live and dead cells according to the manufacture protocol.<sup>19</sup> After incubation for 5 days, the cross section of channeled collagen gels was obtained by cutting it to thin slices (5 mm × 10 mm × 1 mm). Then, the slices were immersed into AO mixture solution and incubated for 10 minutes at 37°C. After stain aspiration, the samples were observed using a fluorescent microscope (Zeiss Axio Observer, ZI). Different sections of collagen gel were imaged to confirm uniform distribution of the cells in the hydrogel. Every sample was characterized for cell viability assay.

MTT assay was also performed to study cell proliferation after 1, 3, and 5 days of seeding HUVECs in the microfluidic hydrogels. In brief, the culture media perfusion was disconnected, and then, MTT solution in DMEM was added to each sample. After 3-hour incubation in 37°C, the MTT solution was replaced with 2-propanol (Sigma, USA) solution comprising 0.01 N HCl to solubilize formazan in viable cells. The absorbance of the solution at 570 nm was measured by using an ELISA reader (Stat Fax-2100, USA).

## 2.6 | Statistical analysis

All obtained data are expressed as the mean ± standard deviation (SD) in all cases. Assessments among different groups of collagen concentrations were performed using 1-way analysis of variance (ANOVA), and *P* values less than 0.05 were considered statistically meaningful.

# 3 | THEORETICAL MODELING

## 3.1 | Governing equations

In this numerical study, the hydrodynamic conditions were modeled by using finite element modeling software (COMSOL Multiphysics ver. 5.3). Fluid flow through the microfluidic hydrogel follows Darcy's law:

$$\nabla P_{\text{hydrogel}} = -\frac{1}{H_{\text{cond}}} v_{\text{hydrogel}} \quad (4)$$

where  $P_{\text{hydrogel}}$  is the fluid pressure,  $v_{\text{hydrogel}}$  is the velocity within the hydrogel, and  $H_{\text{cond}}$  represents the hydraulic conductivity of the microfluidic hydrogel. Fluid flow in the microchannels obeyed steady-state Navier-Stokes equations:

$$\rho(v_{\text{channel}} \cdot \nabla) v_{\text{channel}} = -\nabla P_{\text{channel}} + \mu \nabla^2 v_{\text{channel}} \quad (5)$$

where  $v_{\text{channel}}$  is the fluid velocity in microchannels and  $P_{\text{channel}}$  is the pressures inside the vessels,  $\mu = 1.36$  cP is the viscosity of the culture media at 37°C, and  $\rho = 1$  g/cm<sup>3</sup> is the density of culture media. Diffusion in the microfluidic hydrogels is similar to diffusion in a porous medium. In this model, according to Nicholson model, the diffusion equation can be described as follows<sup>19</sup>:

$$\frac{\partial}{\partial t} C = \hat{D} \nabla^2 C + \frac{s}{\alpha} \quad (6)$$

where  $C$  is the concentration of nutrients,  $s$  is the source density of nutrients,  $\alpha$  is the hydrogel porosity, and  $\hat{D} = D \cdot \hat{K}$  is the effective diffusion coefficient of the hydrogel. The tensor  $\hat{K}$  is a mutual ratio of the hydrogels' tortuosity which

can be simplified as a scalar parameter with an inverse relation with the square of tortuosity for the samples with homogeneous. In addition, the diffusion equation in the extracellular space could be described in a free medium as follows.

In this model, we neglect the term(s) because of lacking source density in the microfluidic system. Because diffusion is generated by concentration gradient within the hydrogel, it obeys from the Brownian motion.

### 3.2 | Assumptions and boundary condition

By fixing the pressure gradient, this model considers a laminar fluid flows within the hydrogel's channels. We assume that the hydrogel has a uniform porous size so that the diffusion coefficient  $\hat{D}$  can be considered to be constant in all over the hydrogel bulks. Moreover, because of having uniform porosity and low pressure gradient, the convection effects were neglected. We consider that the microfluidic hydrogel has high level of permeability and diffusion. We also assume that the cell viability depends on the diffusion of nutrients and cells in the hydrogel consume nutrients proliferate. Diffusion was considered to be 1 dimensional (in the direction of channel diameter), and the nutrient concentration was normalized by dividing concentration at each point by concentration within channel surface. Therefore, the normalized initial concentrations were considered to be 1 within the channel surface and zero on the microfluidic hydrogel's boundaries. We considered a no-flux boundary condition on hydrogel-PMMA interfaces.

## 4 | RESULTS AND DISCUSSION

### 4.1 | Morphology and porosity of microfluidic hydrogel

It is clear that morphology and porosity of the hydrogels play an important role in regulatory of the nutrient delivery and oxygen transport to the cells. Collagen hydrogels with different concentrations (1, 2, and 3 wt%) have been dried under vacuum condition, and microporous constructed were generated. The results of porosity study via liquid displacement method<sup>20</sup> showed that collagen concentration can control the percentage of micro of hydrogels' porosity. The porosity of the samples was determined to be 54%, 35%, and 22% when collagen concentration was 1, 2, and 3 wt% respectively. We identified micropore shape by using a scanning electron microscope (Figure 2A). Figure 2A indicates a relatively homogeneous and interconnected distribution of pores in the hydrogels. Figure 2A shows that the average diameters of pores of the samples with 1, 2, and 3 wt% of collagen were approximately  $197.6 \pm 12.0$ ,  $137.5 \pm 7.6$ , and  $87.35 \pm 9.1$   $\mu\text{m}$  respectively. The results showed that the porosity percentage was linearly decreased with collagen concentrations. Therefore, we can regulate pore sizes and porosities by using different concentrations of collagen.

### 4.2 | Permeability quantification and hydraulic conductivity

We know that nutrient transport and waste metabolite removal which are essential to support cell survival in the hydrogels are regulated by permeability.<sup>21</sup> Thus, precise evaluation of hydrogel permeability is necessary to control nutrient and oxygen delivery to the cells. The permeability of culture media flow in the microfluidic hydrogels was counted by plotting the pressure difference between inlet and outlet of the flow in the channels over time. The results of measuring culture media columns' height difference for different time intervals are presented in Figure 2C. As shown in Figure 2B, we fitted the data within Equation 1 and achieved an  $R^2$  value of 0.98 for 3 samples. The Darcy's permeability is shown in Figure 2C which points out the resistance to the flow because it shows the velocity of reaching the pressure difference of the reservoirs to the equilibrium and tending with an equal pressure difference.

We also calculated hydraulic conductivity using Equation 3, as indicated in Figure 2D. It can be found out that hydraulic conductivity, which explains the ease of medium flow within the hydrogel, decreases from  $8.69 \times 10^{-5}$  to  $7.05 \times 10^{-5}$  (m/second) when collagen concentration increases from 1 to 3 wt%.

### 4.3 | Diffusion results

The success of 3D constructs for tissue engineering application is limited by nutrient diffusion as a major concern in supporting cell viability. Therefore, studying nutrient diffusion inside a hydrogel is a vital asset. The diffusion rates



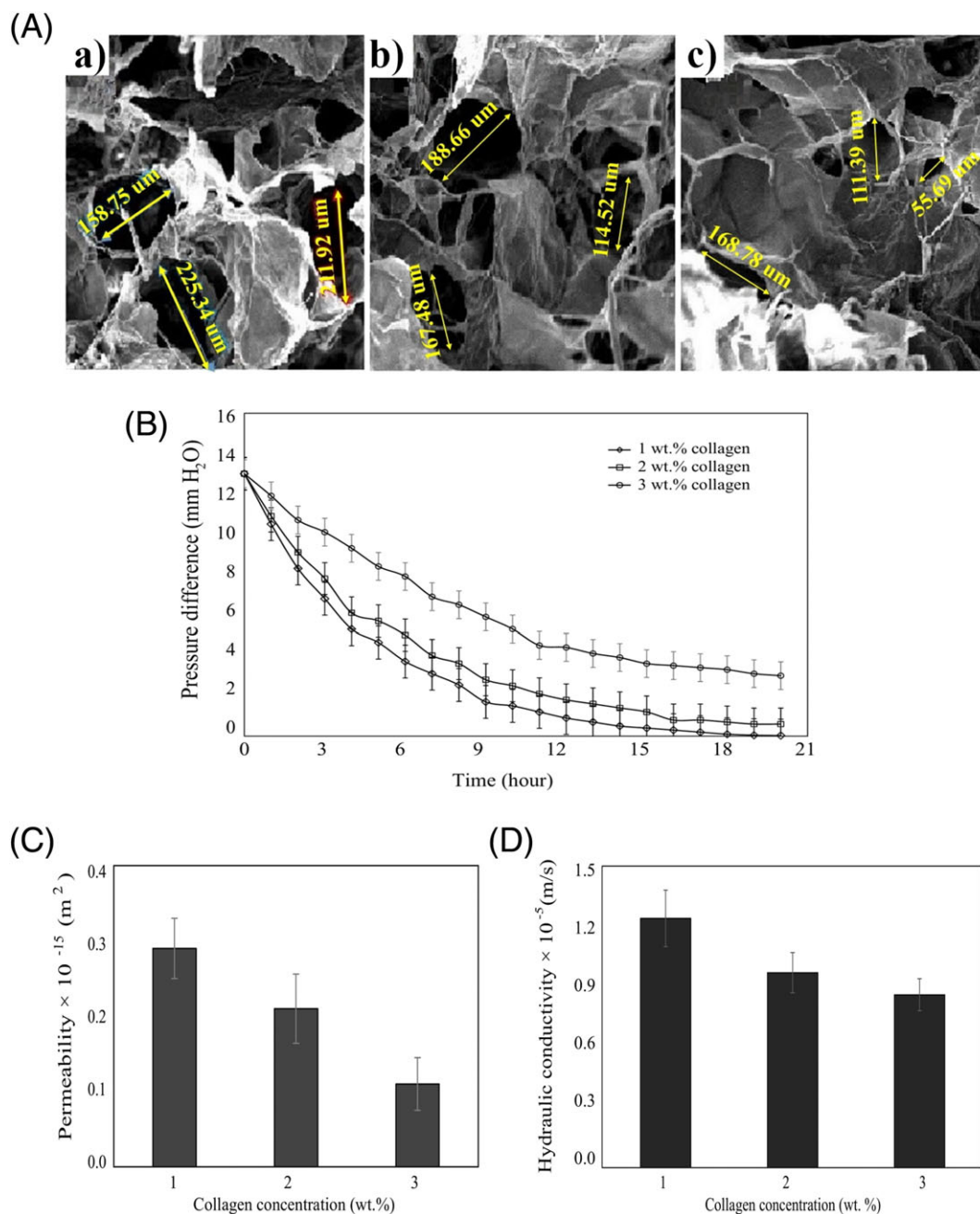


**FIGURE 2** Physical properties of collagen microfluidic hydrogel. A, SEM images of microporosity of collagen gels with different concentrations a, b, and c 1, 2, and 3 wt% respectively. B, Pressure drop over time in microfluidic hydrogels for different concentration of collagen. C, The permeability of 3 collagen gels. D, Hydraulic conductivities of collagen gels

inside collagen gels were studied by using a fluorescent dye (FITC-dextran), and color intensity was obtained via ImageJ software which is shown in Figure 3A to C. In Figure 3A to C, the diffusion profiles of FITC-Dextran and its normalized intensity obtained from ImageJ software were indicated as a function of time for 3 different concentrations of collagen gel. It can be seen that for the sample with collagen concentration of 1 wt%, diffusion patterns were more uniform than 2 other samples due to having more porosity and larger micropores around the channels. Indeed, the diffusion rate enhances gradually with increasing the porosity and pore size of the hydrogel. It also can be found that nutrient concentration declines with distance increase from the microchannel and time.

To define diffusion coefficient, we neglect the convective effects which were emerged due to nonuniform pores and used Nicholson's model<sup>22,23</sup> for the inhomogeneous environment (Equation 5). The diffusion coefficients for different

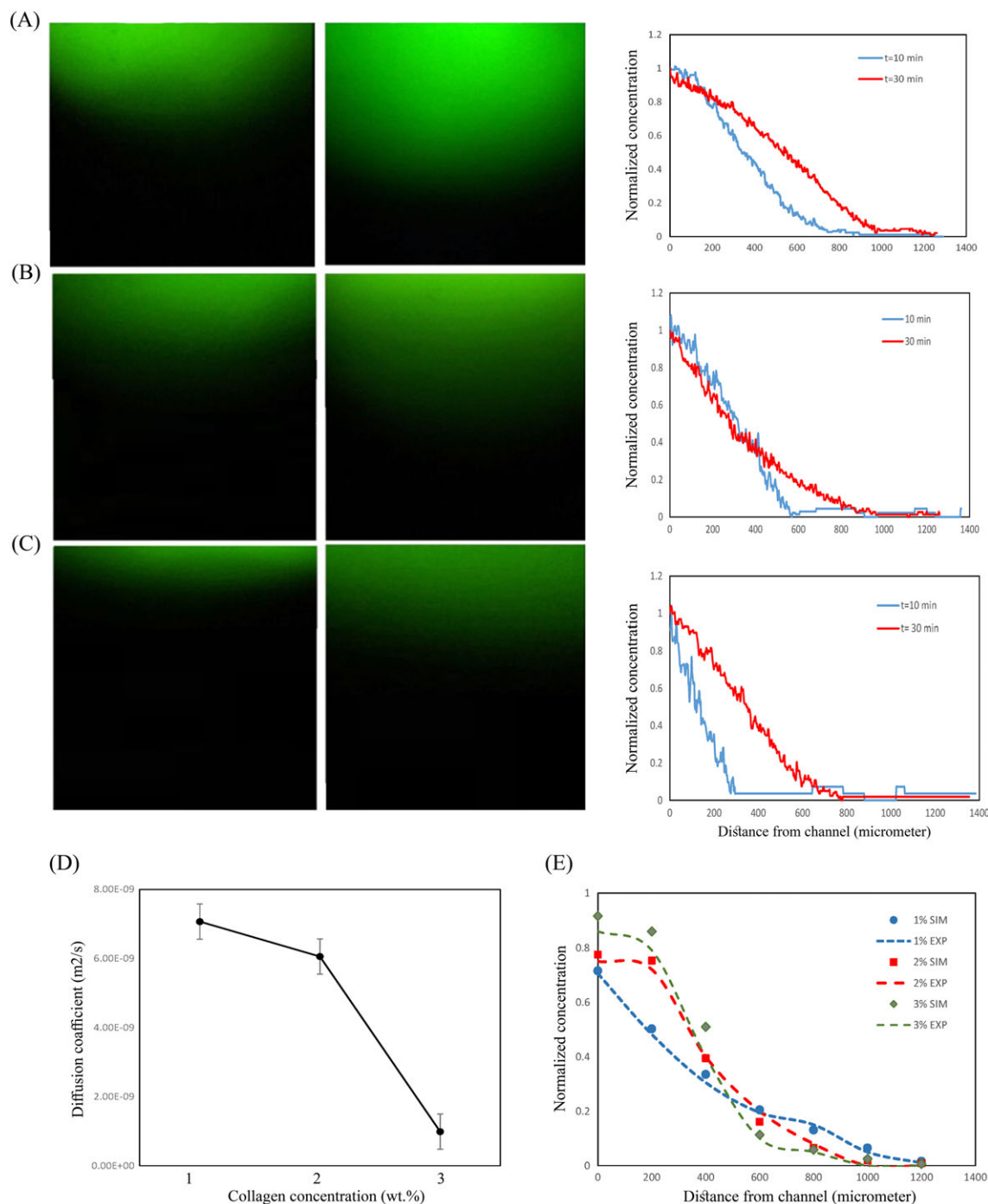


**FIGURE 3** Fluorescent images of diffusion profiles of dextran-FITC and its normalized distribution obtained from ImageJ software for 10 and 30 minutes in the collagen hydrogels with different concentrations (magnification  $\times 10$ ): A, 1%, B, 2%, and C, 3%. D, Diffusion coefficient within the hydrogels obtained by fitting experimental results of fluorescent dye diffusion in Equation 6. E, The experimental (EXP) and simulation (SIM) diffusion profiles of the fluorescent dye in the microfluidic hydrogel with different concentrations of collagen (1–3 wt%) versus distance from microchannels. All of the above data are obtained from experiments and calculations with 5 repetitions

concentrations of collagen can be obtained by fitting the experimental results in Equation 6 (using Mathematica software) (Figure 3D). These results revealed that diffusion velocities increased as collagen concentration decreased due to porosity enhancement. As Figure 3 shows, the diffusion coefficient of FITC-dextran in the samples derived from 1 wt% collagen was nearly 1.4 and 7 times more than that in the samples containing 2 and 3 wt% collagen respectively. These experimental results confirmed the similar patterns of FITC-dextran diffusion in porous media under identical conditions, which was reported in other studies.<sup>22,23</sup>

## 4.4 | Simulation results

We well know that the cell viability within the microfluidic hydrogel is influenced by nutrients and soluble factor diffusion through the hydrogel's bulk. Thus, understanding of nutrient transport in the hydrogel is necessary to interpret the results of cell viability. Therefore, we studied the nutrient dispensations in the microfluidic hydrogel by simulations. To evaluate the effect of the number and size of the microchannels inside the hydrogel, we performed a numerical study by using COMSOL Multiphysics 5.3.

### 4.4.1 | Grid

The geometry of modeled structure was meshed using COMSOL Multiphysics ver. 5.3. A triangle grid was used for the geometry of the microfluidic hydrogel. The number of elements was about 169 259, and the minimum quality of mesh was 0.197. This number of meshes was changed to examine different grid numbers between 169 259 and 1 566 088. We found no significant difference among the obtained results using more than 50 000 cells. Therefore, this number of meshes was used in our simulation.

### 4.4.2 | Concentration distribution

Figure 4A shows the distribution of nutrient concentration for the microfluidic hydrogels with different channel diameters (100, 300, 500  $\mu\text{m}$ ). The parameter of concentration was normalized by dividing it by the nutrient concentration at the surface of the channels which is in direct contact with culture media source. It can be seen that as the channel diameter increases, the diffusion rate of nutrients to further zones from the channels enhances. For example, in the case of  $d = 100 \mu\text{m}$ , we can find a depletion zone with no nutrients (blue zones). This zone decreases when the channel diameter increased to 300 and 500  $\mu\text{m}$ , which means a channel with larger diameter exhibits a higher diffusion rate under an equal pressure gradient. According to the optimum ratio of the microchannel volume to the total volume of the microfluidic hydrogel, the enhancement of channel diameter is limited. As Figure 4C shows when  $d = 500 \mu\text{m}$  although the nutrient diffusion was increased, it is possible that the microfluidic hydrogel cannot stand the perfusion volume of culture media.

Then, we fixed the channel diameter at 300  $\mu\text{m}$  and changed the interchannel distance the number of channels (1, 3, and 5 channels was selected). Figure 4B shows our simulation results of nutrient concentration for the systems containing

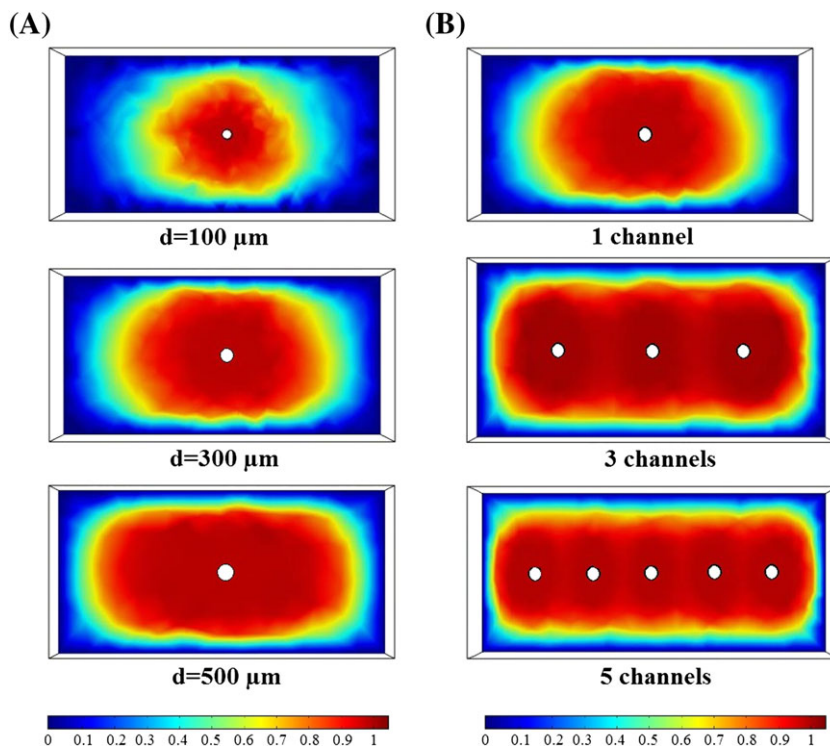


**FIGURE 4** Numerical simulation of microfluidic hydrogel with different diameter and interdistances of channels. A, The distribution of normalized concentration of nutrient or evaluation of the effect of different channel diameter. B, The profile of normalized nutrient concentration as a function of distance among channels



different channel numbers. As this figure indicates, we have enough nutrient diffusion when 3 channels were inserted in the microfluidic hydrogel without depletion zone and the possibility of hydrogel collapse.

Moreover, it is well known that the porous media of the gel provides much more resistance to flow than channels. However, when channel's diameter becomes too large, the efficiency of nutrient transport decreases due to the rapid media outflow which leads to a rapid drop in pressure gradient on both sides of the gel and finally flow cessation when the nutrients are not penetrated inside the porous medium uniformly. To analysis of nutrient transport more accurately, we defined the degree of coverage by dividing the volume of the gel containing a nutrient concentration higher than 80% of that in inlet medium flow. Table 1 shows the degree of nutrient coverage for different channels' diameter and channels' distance. As expected, the device with a 100- $\mu\text{m}$  channel diameter indicates insignificant coverage during 3600 seconds. However, 2 other samples provided coverage degree more than 50% which shows that during 3600 seconds, more than 50% of hydrogel volume contain at least 80% of nutrient concentration in inlet flow. It also can be found out that there is no meaningful difference between the 2 devices containing channel diameter of 300 and 500  $\mu\text{m}$  ( $P$  value  $>0.05$ ). Therefore, in order to avoid the risk of the rapid pressure drop and flow-stop that occur for larger channels, the sample with a channel of 300- $\mu\text{m}$  diameter can be a more careful choice.

From the results of Table 1, it also can be implied that the devices with the channel with smaller diameter reach to equal coverage degree in longer time in comparison with the samples containing larger channel diameter. Thus, using larger channels provides more rapid supply of the nutrients inside the hydrogels. However, the high rate of diffusion alone is not adequate for the assessment of the practical operation of the microfluidic systems. It is also important to obtain the efficiency of nutrient transport through the hydrogel media with minimum loss of pressure gradient. From simulation results, we obtain the efficiency of a channel size and number as the following equation:

$$\text{Efficiency (\%)} = \frac{\text{Nutrient amount in gel}}{\text{Average of inlet nutrient}} \times 100 \quad (7)$$

The efficiencies of the microfluidic hydrogel with different channel number and channels' diameter are presented in Table 1. For the same time duration ( $t = 3600$  seconds), microchanneled hydrogel with 100 channels' diameter had a low efficiency (24%) and the efficiency of the microfluidic device with the 500- $\mu\text{m}$  channels' diameter is a little higher than that of the device with 300  $\mu\text{m}$ . Moreover, the sample with 5 microchannels had an efficiency (64.7) slightly larger than the sample with 3 channels due to rapid medium flows through the channels. Consequently, the hydrogel with 3 microchannels of 300  $\mu\text{m}$  in diameter can provide high diffusion rate and appropriate efficiency without the problems of keeping the continuous flow than other hydrogels.

#### 4.4.3 | The result of velocity and shear stress

In this study, the Navier-Stokes equations were solved to describe the flow within the microchannels. As shown in Figure 5A, for equal initial pressure drop, the highest average velocity (about 95  $\mu\text{m}/\text{second}$ ) was observed in channel diameter of 500  $\mu\text{m}$ . It can be elucidated by the fact that the highest resistance exists on the surface and so flow go more easily in the microchannel with larger cross section (larger diameter). Average velocity was estimated up to 35  $\mu\text{m}/\text{second}$  in the narrowest microchannels (100  $\mu\text{m}$  in diameter), and about 85  $\mu\text{m}/\text{second}$  in the channel diameter of 300  $\mu\text{m}$ . In comparison with some studies which reported that physiological blood flow velocity in vivo was ranging from 84  $\mu\text{m}/\text{second}$  to 1.6 mm/second depending on the vessel type, flow rate in the samples containing channel diameter of 300 and 500  $\mu\text{m}$  can mimic in vivo condition precisely.<sup>24,25</sup>

**TABLE 1** The simulation evaluation of coverage degree and the efficiency of the microfluidic hydrogels

|                                     |     | Coverage Degree (%) | Efficiency (%) |
|-------------------------------------|-----|---------------------|----------------|
| Channels diameter ( $\mu\text{m}$ ) | 100 | 0.28                | 24             |
|                                     | 300 | 0.53                | 42.4           |
|                                     | 500 | 0.61                | 48.8           |
| Channels number                     | 1   | 0.53                | 42.4           |
|                                     | 3   | 0.82                | 56.2           |
|                                     | 5   | 0.93                | 64.7           |

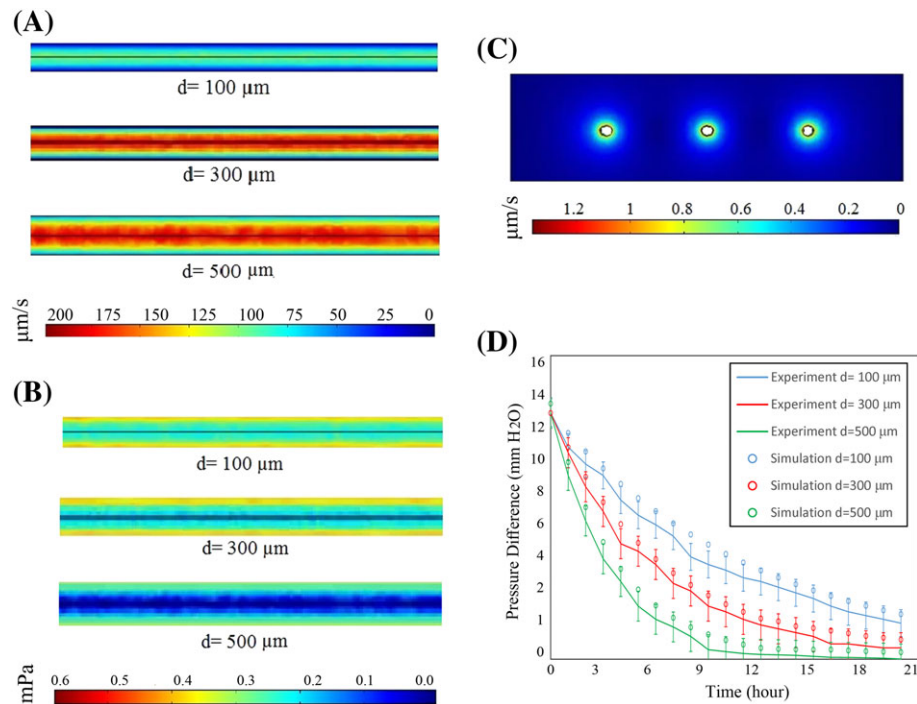


**FIGURE 5** The result of simulation study for velocity and shear stress. A, A 2D distribution of the Navier-Stokes equation was modeled from inside of microchannels. B, The distribution of shear stress in the channels. C, The distribution of Darcy velocity magnitude within the hydrogel bulk. D, The comparison between numerical and experimental results of pressure difference between input and output reservoirs for collagen hydrogels (2 wt% collagen) containing 1 channel with different diameters

It was reported that steady shear stress is one of the external stimuli which contributes in the signal transduction of the cells.<sup>26</sup> It also can be considered as the main parameter in cell migration (an important step for vascularization). Therefore, controlling the shear stresses generated by the microfluidic flow can regulate vascularization tissue engineering constructs.<sup>27</sup>

Moreover, it was obtained that shear stress of 0.5 to 1.5 Pa is needed on cells for endothelial cells to grow well.<sup>28</sup> Excessive values of shear stress may hurt the cell membrane, and compromise cell viability. This negative effect of shear stress can be eliminated by reducing the flow rate and in consequence shear stress. Figure 5B indicates shear stress distribution as a result of surface resistance. The largest and weakest shear stress on the surface were observed in the channels diameter of 100 and 500  $\mu\text{m}$  with a value of about 0.4 and 0.13 mPa respectively. These results showed that shear stress influence on cellular behavior can be ignored. In order to increase the amount of shear stress, the amount of flow rate should be increased.

Furthermore, the Darcy velocity was obtained from simulation results and presented in Figure 5C. It shows that maximal value of velocity in the hydrogel bulk was predicted 1.4  $\mu\text{m}/\text{second}$  near the channel surface as shown in Figure 5C. The reason of significant reduction of velocity within the microfluidic gels in comparison with velocity in the microchannels is the resistance of the hydrogel.

To validate simulation results, pressure difference changes versus time is presented in Figure 5D. It can be seen as the channel diameter increases, the pressure difference between the 2 input and output reservoirs decreases faster due to the higher flow rate. Therefore, in microfluidic hydrogels containing channels diameter of 500  $\mu\text{m}$ , the flow rate will be stopped after 12 hours. Therefore, in a microfluidic system containing channel with a diameter of 500  $\mu\text{m}$ , the flow will be stopped in less than 12 hours, which means the need to readjust the pressure difference and the handling of the system, which provides more problems in controlling the perfusion. Moreover, from a comparison of experimental and numerical results, a good agreement can be observed clearly which shows the simulation results are valid.

#### 4.5 | Cell viability and proliferation

Cell viability is controlled by the diffusion rate of nutrients from microchannels to the encapsulated cells within the collagen gel. To study the effect of channel diameter and their distance on cell number and cell viability, we performed a

live/dead test for microfluidic hydrogel (2wt% collagen) with different channel geometry. Figure 6A,B indicates fluorescent images of stained cells by calcein-AM/4  $\mu$ M EthD-1 of the microfluidic systems at a distance of 500  $\mu$ m of the channels after 1 and 5 days of seeding in the samples with a different number of channels. To investigate the influence of channel diameter on HUVEC viability, we created only 1 channel in each microfluidic system with the diameter of 100, 300, and 500  $\mu$ m and the results are shown in Figure 6A. As Figure 6A shows, no important difference can be

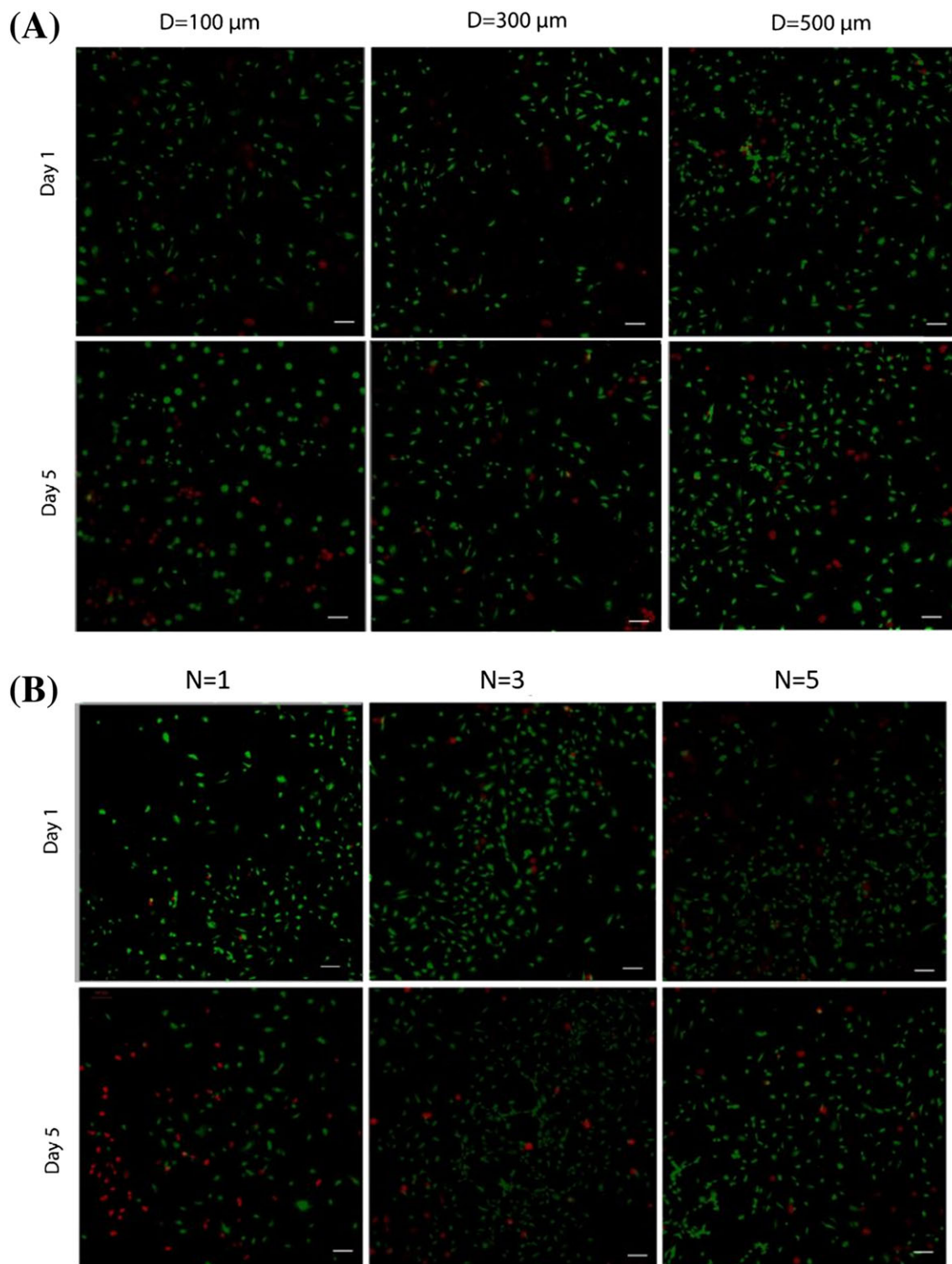


**FIGURE 6** Fluorescent images of the cell viability of HUVECs from the samples after 1 and 5 days for A, the effect of channel diameter and B, the effect of channels number on cell viability. (Scale bar is 100  $\mu$ m)

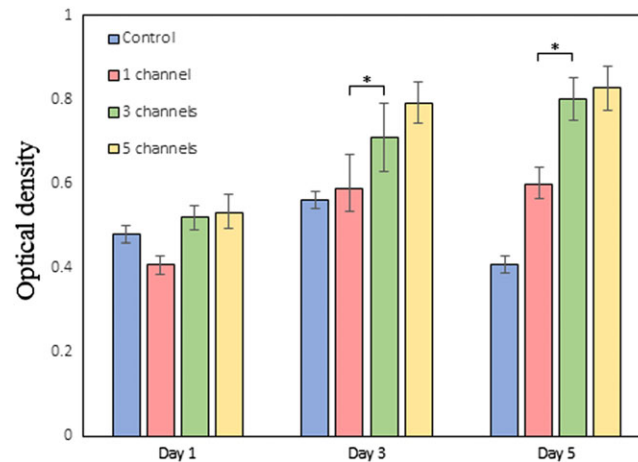


**FIGURE 7** The results of MTT assay of HUVECs seeded inside collagen gel containing different number of microchannels in comparison with static condition. All of these data was attained at least 3 times for every sample (\* $P < 0.05$ )

observed among the samples. This can be due to the lack of effective transfer of culture media to the cells. This will be further supported when Figure 6A indicates that the number of dead cells on day 5 was significantly increased for all specimens. As Figure 6B shows, the enhancement of channel number increases live cell numbers. These results confirm the simulation data because simulation results indicated that there is no significant depletion zone in the samples containing 3 and 5 channels (Figure 4B). This phenomenon also can be seen in Figure 6B. It can be found that there is no significant difference between the samples containing 3 and 5 channels. Therefore, in order to support collagen bulk exposed to perfusion, it is much better to select the specimen with 3 channels as the optimum sample.

Figure 7 indicates the quantitative study of cell viability of the microfluidic hydrogel in comparison with the static condition. We found that HUVEC viability was maximized in the samples with 5 channels (near to 0.8) and reduced to 0.4 in static condition (as control) after 5 days. Although the results indicate that the highest cell viability was observed in the sample with 5 channels, this specimen did not show a meaningful difference in cell growth in comparison with the sample with 3 channels. Moreover, it has main problems in controlling the continuous flow rate and keeping its bulk with less handling. There is also a significant difference between samples with 1 and 3 channels. In fact, optical density in the sample with 3 channels is 1.36 times larger than the sample with 1 channel. Because in the system with 1 channel, as the simulation results showed (Figure 4), there are more depletion regions in which cells died due to lack of delivering enough nutrients. Subsequently, in the microfluidic hydrogels with 3 channels of 300- $\mu\text{m}$  diameter, higher cell viability can be observed due to a more uniform nutrient concentration and controllable and continuous perfusion rate during 5 days. Our results showed a major increase compared to previous studies, which reported about 60% cell viability for day 5.<sup>10,29,30</sup>

## 5 | CONCLUSION

We have designed a microfluidic cell-laden hydrogel of collagen with different concentrations and found the optimum concentration based on suitable porosity, and permeability. Then, we studied the effect of channel diameter and their interdistance to stabilize and optimize perfusion rate and nutrient diffusion in microfluidic hydrogel using COMSOL software. The results demonstrated that microfluidic systems with 3 channels of 300  $\mu\text{m}$  in diameter had a controllable rate of perfusion and appropriate diffusion during 5 days of culturing. The simulation results of permeability were compared with experimental data, and a good agreement was observed. Therefore, using numerical study can be potentially helpful to design a suitable microfluidic system and engineer functional synthetic tissues with clinical applications in regenerative medicine.

## ACKNOWLEDGEMENT

The authors express special thanks to Iranian National Science Foundation (INSF) for the financial support and great assistance in this research project.



## ORCID

Zeinab Salehi  <http://orcid.org/0000-0002-3541-7530>

## REFERENCES

1. Zheng Y, Henderson PW, Choi NW, Bonassar LJ, Spector JA, Stroock AD. Microstructured templates for directed growth and vascularization of soft tissue in vivo. *Biomaterials*. 2011;32(23):5391-5401.
2. Zhong M, Wei D, Yang Y, et al. Vascularization in engineered tissue construct by assembly of cellular patterned micro-modules and degradable microspheres. *ACS Appl Mater Interfaces*. 2017.
3. Park J, Berthiaume F, Toner M, Yarmush ML, Tilles AW. Microfabricated grooved substrates as platforms for bioartificial liver reactors. *Biotechnol Bioeng*. 2005;90(5):632-644.
4. Kayabölen A, Keskin D, Aykan A, Karshoğlu Y, Zor F, Tezcaner A. Native extracellular matrix/fibroin hydrogels for adipose tissue engineering with enhanced vascularization. *Biomed Mater*. 2017;12(3):035007.
5. He J, Chen R, Lu Y, et al. Fabrication of circular microfluidic network in enzymatically-crosslinked gelatin hydrogel. *Mater Sci Eng C*. 2016;59:53-60.
6. Bertassoni LE, Cecconi M, Manoharan V, et al. Hydrogel bioprinted microchannel networks for vascularization of tissue engineering constructs. *Lab Chip*. 2014;14(13):2202-2211.
7. Goldman SM, Barabino GA. Cultivation of agarose-based microfluidic hydrogel promotes the development of large, full-thickness, tissue-engineered articular cartilage constructs. *J Tissue Eng Regen Med*. 2014.
8. Chrobak KM, Potter DR, Tien J. Formation of perfused, functional microvascular tubes in vitro. *Microvasc Res*. 2006;71(3):185-196.
9. Sakaguchi K, Shimizu T, Horaguchi S, et al. In vitro engineering of vascularized tissue surrogates. *Sci Rep*. 2013;3(1):1316.
10. Song YS, Lin RL, Montesano G, et al. Engineered 3D tissue models for cell-laden microfluidic channels. *Anal Bioanal Chem*. 2009;395(1):185-193.
11. Deakin A. Model for initial vascular patterns in melanoma transplants. *Growth*. 1976;40(2):191-201.
12. Cioffi M, Boschetti F, Raimondi MT, Dubini G. Modeling evaluation of the fluid-dynamic microenvironment in tissue-engineered constructs: a micro-CT based model. *Biotechnol Bioeng*. 2006;93(3):500-510.
13. Hutmacher DW, Singh H. Computational fluid dynamics for improved bioreactor design and 3D culture. *Trends Biotechnol*. 2008;26(4):166-172.
14. Provin C, Takano K, Sakai Y, Fujii T, Shirakashi R. A method for the design of 3D scaffolds for high-density cell attachment and determination of optimum perfusion culture conditions. *J Biomech*. 2008;41(7):1436-1449.
15. Shi Y. Numerical simulation of global hydro-dynamics in a pulsatile bioreactor for cardiovascular tissue engineering. *J Biomech*. 2008;41(5):953-959.
16. Lawrence BJ, Devarapalli M, Madhally SV. Flow dynamics in bioreactors containing tissue engineering scaffolds. *Biotechnol Bioeng*. 2009;102(3):935-947.
17. Sudo R, Chung S, Zervantonakis IK, et al. Transport-mediated angiogenesis in 3D epithelial coculture. *FASEB J*. 2009;23(7):2155-2164.
18. Wong KH, Truslow JG, Tien J. The role of cyclic AMP in normalizing the function of engineered human blood microvessels in microfluidic collagen gels. *Biomaterials*. 2010;31(17):4706-4714.
19. Nicholson C. Diffusion and related transport mechanisms in brain tissue. *Rep Prog Phys*. 2001;64(7):815-884.
20. Lee Y, Jeong J, Youn I, Lee W. Modified liquid displacement method for determination of pore size distribution in porous membranes. *J Membr Sci*. 1997;130(1-2):149-156.
21. O'Brien FJ, Harley BA, Waller MA, Yannas IV, Gibson LJ, Prendergast PJ. The effect of pore size on permeability and cell attachment in collagen scaffolds for tissue engineering. *Technology and Health Care: Official Journal of the European Society for Engineering and Medicine*. 2007;15(1):3-17.
22. Nicholson C, Tao L. Hindered diffusion of high molecular weight compounds in brain extracellular microenvironment measured with integrative optical imaging. *Biophys J*. 1993;65(6):2277-2290.
23. Thorne RG, Nicholson C. In vivo diffusion analysis with quantum dots and dextrans predicts the width of brain extracellular space. *Proc Natl Acad Sci*. 2006;103(14):5567-5572.
24. Leclerc E, El Kirat K, Griscom L. In situ micropatterning technique by cell crushing for co-cultures inside microfluidic biochips. *Biomed Microdevices*. 2008;10(2):169-177.
25. Maksan S-M, Zilfi Ülger MMG, Schmidt J. Impact of antithrombin III on hepatic and intestinal microcirculation in experimental liver cirrhosis and bowel inflammation: an in vivo analysis. *World J Gastroenterol: WJG*. 2005;11(32):4997-5001.
26. Frangos J, McIntire L, Eskin S. Shear stress induced stimulation of mammalian cell metabolism. *Biotechnol Bioeng*. 1988;32(8):1053-1060.



27. Kan P, Miyoshi H, Yanagi K, Ohshima N. Effects of shear stress on metabolic function of the co-culture system of hepatocyte/nonparenchymal cells for a bioartificial liver. *ASAIO Journal (American Society for Artificial Internal Organs: 1992)*. 1997;44:M441-M444.
28. Wong AP, Perez-Castillejos R, Love JC, Whitesides GM. Partitioning microfluidic channels with hydrogel to construct tunable 3-D cellular microenvironments. *Biomaterials*. 2008;29(12):1853-1861.
29. Khademhosseini A, Yeh J, Jon S, et al. Molded polyethylene glycol microstructures for capturing cells within microfluidic channels. *Lab Chip*. 2004;4(5):425-430.
30. Ling Y, Rubin J, Deng Y, et al. A cell-laden microfluidic hydrogel. *Lab Chip*. 2007;7(6):756-762.

**How to cite this article:** Jafarkhani M, Salehi Z, Shokrgozar MA, Mashayekhan S. An optimized procedure to develop a 3-dimensional microfluidic hydrogel with parallel transport networks. *Int J Numer Meth Biomed Engng*. 2019;35:e3154. <https://doi.org/10.1002/cnm.3154>